ELSEVIER

International Journal of Solids and Structures 41 (2004) 4889–4898

INTERNATIONAL JOURNAL OF SOLIDS and STRUCTURES

www.elsevier.com/locate/ijsolstr

Analysis of electrostatic comb-driven actuators in linear and nonlinear regions

Michael M. Tilleman *

GalayOr, Inc., 1 Yodfat Street, P.O. Box 1351, Lod 71100, Israel

Received 12 April 2004; received in revised form 12 April 2004
Available online 25 May 2004

Abstract

Comb-drive actuators have become a standard component of MEMS devices. Though their characteristic behavior has been investigated extensively over the last decade, their controllable motion has been limited to the linear region of the normalized electrostatic force. In this paper an analytical solution for the actuator displacement is presented, arrived at by the Schwartz–Christoffel mapping. Resulting in a simple formula the solution enables the extension of the usable dynamic range of a comb-drive actuator to include the nonlinear zone.

Keywords: Actuator; MEMS; Comb-drive; Electrostatic; Conformal mapping

1. Introduction

Comb-drive actuators operating on electrostatic force have become a classic component in MEMS devices. Their application spans the range from linear actuation (Tang et al., 1990), through rotational actuation (Sniegowski and Garcia, 1996), accelerometry (Yun et al., 1992), scanning probes (Yao et al., 1992), gyroscopes (Pisano, 1989), RF filtering (Wang and Nguyen, 1999) and microgripping (Kim et al., 1990). It is natural, therefore, that considerable interest and effort have been invested in their improvement. The case is always how to minimize the size of the device yet fully control its motion, preferably under the smallest electric field. Thus, several groups presented analyses and ways of optimally designing comb-drive actuators, for instance Ye et al. (1998) and Jensen et al. (2001).

Conformal mapping is an important technique used in the analysis of electromagnetic fields, including integrated electrooptical structures (Goano et al., 2001). Particularly for the case of interdigitated capacitors circumventing polygonal regions the Schwartz–Christoffel (SC) formula, a special conformal transformation, is applicable. While an analytical approach is suitable for a limited number of geometrical patterns, a more general, numerical tool has become standard for design purposes (Driscoll, 1996, 1999).

* Tel.: +972-3-544-9191; fax: +972-3-544-9111.
E-mail addresses: mtilleman@hotmail.com, mik012@go.com (M.M. Tilleman).

0020-7683/$ - see front matter © 2004 Elsevier Ltd. All rights reserved.
doi:10.1016/j.ijsolstr.2004.04.034

Still, even the analytically solvable simple cases may lend themselves to predict the electrostatic forces exerted in comb-drives (Brown and Churchill, 1995).

The objective of this paper is to solve analytically the problem of the electrostatic force driving a comb-drive actuator. Suggested further is that the algebraic expression for the electrostatic driving force will permit controlling the actuator motion over an extended range, beyond the traditionally used linear range. In this manner, the developed model is useful to predict the instability of comb-drive actuators in the nonlinear condition.

2. Theory

2.1. Description of the problem and its reduction

The problem before us is that of electrostatic force acting on a dielectric body, moving fingers of a comb-drive actuator. The geometrical complexity of the comb-drive structure, illustrated in Fig. 1a, can be reduced to a two dimensional problem due to the fixed fingers positive charge, and the moving fingers and substrate zero charge, illustrated in Fig. 1b. The problem can be further reduced, owing to symmetry, to some basic building blocks represented by a single moving and fixed finger, represented by the cell in Fig. 1c. Another simplification is attained by selecting the part enclosed in the broken box in Fig. 1c, thus producing the patterns shown in Fig. 1d, then in turn in Fig. 1e. Thus one arrives at a few elemental structures (see Fig. 1d and e) which while being solvable, represent the entire complex.

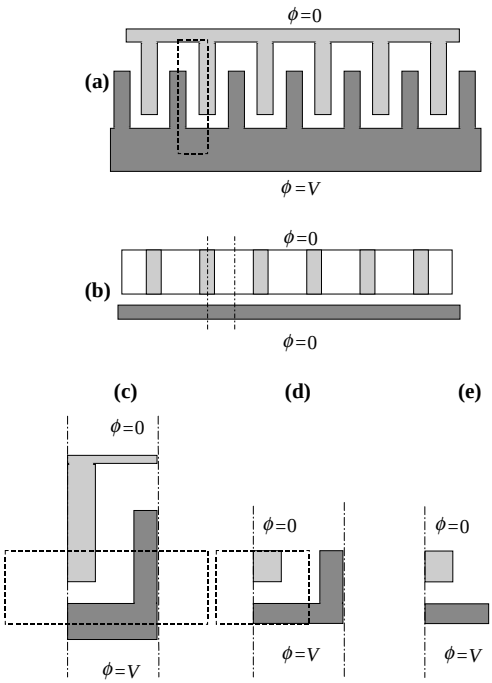

Fig. 1. Schematic of a comb-drive configuration: (a) in the horizontal plane, (b) in the vertical plane, (c) detail defined by the broken-line rectangle in (a), (d) detail defined by the broken-line rectangle in (c), and (e) detail defined by the broken-line rectangle in (d).

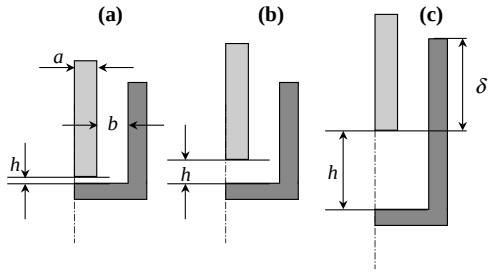

Fig. 2. Three positions of the moving finger relative to the comb-drive stator: (a) case 1: finger very close to stator base, (b) case 2: finger distance from stator base equal to the gap between the moving and fixed finger, and (c) case 3: finger very far from stator relative to the gap.

The electrostatic field of interest lies between the moving and fixed finger. It is formally defined by boundary values and a governing Laplace equation, i.e. $\nabla^2\phi = 0$, where ϕ is the electrostatic potential. The polygonal yet complex geometry renders the problem conveniently solvable by conformal transformation, thus mapping it onto a plane where it can be expressed in a simple, canonical form. For the polygonal geometry the transformation of choice is of the Schwartz–Christoffel type. Thus one begins by establishing a $\mathrm{d}w/\mathrm{d}z$ expression, leading to the mapping of the w $(= u + \mathrm{i}v)$ plane domain containing the pattern of interest to a z $(= x + \mathrm{i}y)$ plane. The mapping of any shape in this manner produces a domain containing the entire upper half of the z plane. In turn the z plane is transformed to the canonical η plane, where the domain of interest is mapped to an infinite strip. Thus found is a solution for the potential as a function of η $(= \xi + \mathrm{i}\psi)$, which is traced back to its equivalent in w.

Based on their adequate representation of the physical problem, three simple cases were selected to model the motion of a comb-drive. Though each pertains to a certain range within the moving-finger path, together they describe the moving finger at any location within the fixed array. Fig. 2 illustrates the three cases where: (a) is the region very close to the stator base relative to the gap it forms with the fixed finger, (b) the distance of the moving finger from the stator base equals the gap, and (c) the moving finger is far from the stator base relative to the gap.

2.2. Solution

2.2.1. Case 1

Assuming a moving finger with a width of $2a$ distanced at h from the fixed base, as shown in Fig. 2a, the plane w maps to the upper half of a plane z via the Schwartz–Christoffel derivative $\mathrm{d}w/\mathrm{d}z$, as

$$\frac{\mathrm{d}w}{\mathrm{d}z} = B\frac{\sqrt{z+1}}{z}, \tag{1}$$

where B is a constant. Assuming values of $w = 0$ at $z = -1$, i.e. the origin of w lies at the tip of the moving finger, as depicted in Fig. 1e the integral of Eq. (1) is

$$w(u,v) = \frac{2}{\pi}h\left[\sqrt{z+1} - \tanh^{-1}(\sqrt{z+1})\right]. \tag{2}$$

Determined by the geometry B becomes h/π. The map in plane z is shown in Fig. 3a. Note that the boundary values apply such that $\phi = 0$ at $z < 0$, and $\phi = V$ at $0 < z$. The mapping to plane η is accomplished via $\eta = \ln(z)$, thus forming an infinite strip as shown in Fig. 3c. The boundary values apply such

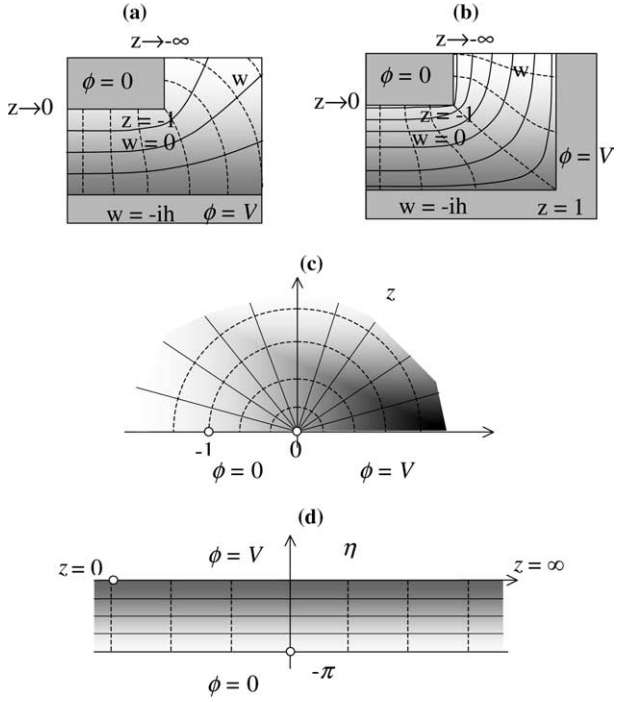

Fig. 3. Conformal transformation of the polygon (a) in the w plane, to the upper half-plane in z (b), and an infinite strip in η (c).

that $\phi = 0$ at $\mathrm{Im}(\eta) = -\pi$ and $\phi = V$ at $\mathrm{Im}(\eta) = 0$. The field potential is obtained by solving the governing Laplace equation in the η plane:

$$\phi(\eta) = V\left[1 + \frac{\mathrm{Im}(\eta)}{\pi}\right]. \tag{3}$$

Once the derivative $\mathrm{d}w/\mathrm{d}z$ is solved producing the mapping transformations of Eq. (2) and the second transformation to plane η is accomplished via $\eta = \ln(z)$, the field potential is produced by the inverse transformation:

$$\phi(z) = V\left\{1 + \frac{\mathrm{Im}[\ln(z)]}{\pi}\right\} \quad \text{and} \quad \phi(w) = V\left\{1 + \frac{\mathrm{Im}[\ln(g[w])]}{\pi}\right\}, \tag{4}$$

here g is the implicit function of w, i.e. reciprocal to the function in Eq. (2), such that $z = g(w)$.

The electrostatic distributed force at the surface is determined by

$$f = -\frac{1}{2\varepsilon}q^2\hat{n} = -\frac{1}{2}\varepsilon\left[\frac{\partial\phi(w)}{\partial n}\right]^2\hat{n}, \tag{5}$$

where q is the electric charge, ε is the permittivity and $\hat{n}$ is a unit vector normal to the surface. The potential gradient is expressed as

$$\frac{\partial\phi(w)}{\partial n} = \frac{\partial\phi(w)}{\partial u} + \mathrm{i}\frac{\partial\phi(w)}{\partial v} = \mathrm{Re}\left[\frac{\partial\phi(w)}{\partial w}\right] + \mathrm{i}\,\mathrm{Im}\left[\frac{\partial\phi(w)}{\partial w}\right]. \tag{6}$$

Next

$$\frac{\partial\phi(w)}{\partial w}=\frac{\partial\,\mathrm{Im}\{\ln[g(w)]\}}{\partial w}=\frac{\partial\,\mathrm{Im}[\ln(z)]}{\partial z}\frac{\mathrm{d}z}{\mathrm{d}w}. \tag{7}$$

In the last term one identifies at the right hand side the inverse Schwartz–Christoffel derivative $\mathrm{d}w/\mathrm{d}z$. With some algebra the derivative in z becomes remarkably simple, expressed as

$$\frac{\partial\,\mathrm{Im}[\ln(z)]}{\partial z}=\frac{\partial}{\partial z}\tan^{-1}\left(\frac{y}{x}\right)=-\frac{1}{1+\left(\frac{y}{x}\right)^2}\left(\frac{y}{x^2}+\mathrm{i}\frac{1}{x}\right)=-\mathrm{i}\frac{1}{z}. \tag{8}$$

Consequently the potential gradient is

$$\mathrm{Re}\left[\frac{\partial\phi(w)}{\partial w}\right]=-\frac{V}{\pi}\mathrm{Re}\left(\mathrm{i}\frac{1}{\sqrt{z+1}}\right)=\frac{V}{\pi}\begin{cases}0, & -1\leqslant z<0;\\ \dfrac{1}{\sqrt{-1-z}}, & z<-1\end{cases} \tag{9}$$

and

$$\mathrm{Im}\left[\frac{\partial\phi(w)}{\partial w}\right]=-\frac{V}{\pi}\mathrm{Im}\left(\mathrm{i}\frac{1}{\sqrt{z+1}}\right)=\frac{V}{\pi}\begin{cases}\dfrac{1}{\sqrt{1+z}}, & -1\leqslant z<0;\\ 0, & z<-1.\end{cases} \tag{10}$$

Substituting these expressions in Eq. (4) results in the following distributed force density:

$$f=\frac{\varepsilon}{2}\left(\frac{V}{\pi}\right)^2\begin{cases}\mathrm{i}\dfrac{1}{1+z}, & -1\leqslant z<0;\\ -\dfrac{1}{1-z}, & z<-1.\end{cases} \tag{11}$$

The total force per thickness acting along the surface in the direction of motion is the integral over the surface; from $w=a$ to $\mathrm{i}H$, where a is half the rod width and H is the finger length. The evaluation of the force along the surface begins with integrating the distributed force density over w, then transforming to the z plane:

$$\begin{aligned}F&=\frac{\varepsilon}{2}\left(\frac{V}{\pi}\right)^2\left(-\mathrm{i}\int_a^0\frac{1}{1+z}\,\mathrm{d}w+\int_0^{\mathrm{i}H}\frac{1}{z+1}\,\mathrm{d}w\right)\\&=\frac{\varepsilon}{2}\left(\frac{V}{\pi}\right)^2\left(-\mathrm{i}\int_{-z_0}^{-1}\frac{1}{1+z}\frac{\mathrm{d}w}{\mathrm{d}z}\,\mathrm{d}z+\int_{-1}^{-\infty}\frac{1}{z+1}\frac{\mathrm{d}w}{\mathrm{d}z}\,\mathrm{d}z\right).\end{aligned} \tag{12}$$

The term $(z+1)^{-1}$ in the integrand can be replaced by the expression $\left(\frac{B\,\mathrm{d}z}{z\,\mathrm{d}w}\right)^2$ derived from Eq. (1), thus the force integral can be rewritten as

$$
\begin{aligned}
F &= \frac{\varepsilon}{2}(hV)^2\left(-\mathrm{i}\int_a^0\left(\frac{B\,\mathrm{d}z}{z\,\mathrm{d}w}\right)^2\mathrm{d}w+\int_0^{\mathrm{i}H}\left(\frac{B\,\mathrm{d}z}{z\,\mathrm{d}w}\right)^2\mathrm{d}w\right)\\
&= \frac{\varepsilon}{2}\left(\frac{V}{\pi}\right)^2\left(-\mathrm{i}\int_{-z_0}^{-1}\frac{\mathrm{d}z}{z^2\,\mathrm{d}w}\,\mathrm{d}z+\int_{-1}^{-\infty}\frac{\mathrm{d}z}{z^2\,\mathrm{d}w}\,\mathrm{d}z\right)\\
&= \frac{\varepsilon}{2}\left(\frac{V}{\pi}\right)^2\frac{1}{B}\left(-\mathrm{i}\int_{-z_0}^{-1}\frac{\mathrm{d}z}{z\sqrt{z+1}}+\int_{-1}^{-\infty}\frac{\mathrm{d}z}{z\sqrt{z+1}}\right)\\
&= \frac{\varepsilon V^2}{2\pi h}\left(-\mathrm{i}\ln\frac{\sqrt{z+1}-1}{\sqrt{z+1}+1}\bigg|_{-z_0}^{-1}+\ln\frac{\sqrt{z+1}-1}{\sqrt{z+1}+1}\bigg|_{-1}^{-\infty}\right)\\
&= \frac{\varepsilon V^2}{2\pi h}\left(\pi-\mathrm{i}\ln\frac{1-\sqrt{1-z_0}}{1+\sqrt{1-z_0}}\right).
\end{aligned}
\tag{13}
$$

Note that similarly the potential gradient may be expressed as

$$
\frac{\partial\phi(w)}{\partial n(w)}=\frac{V}{\pi}\left(\frac{\mathrm{d}z}{z\,\mathrm{d}w}\right)\bigg|_{\text{surface}}. \tag{14}
$$

The integrand $\left(\frac{\mathrm{d}z}{z^2\,\mathrm{d}w}\right)\mathrm{d}z$ allows deriving the total force for any given geometry, since the term $\mathrm{d}z/\mathrm{d}w$ is defined either by Eq. (1) or another Schwartz–Christoffel derivative.

From the result of Eq. (13) the normalized force becomes

$$
2\frac{Fh}{\varepsilon V^2}=1-\mathrm{i}\frac{1}{\pi}\ln\frac{1-\sqrt{1-z_0}}{1+\sqrt{1-z_0}}, \tag{15}
$$

where z_0 of the z plane corresponds to a in the w plane, determined by Eq. (2). Considering that the analysis is carried out for half a moving finger, the resulting normalized force is doubled, as expressed in Eq. (15). It contains a component dependent on z_0 in the negative direction of v, and a constant component in the positive direction of u. The latter is a unity, identical to a direct solution of the finger-capacitor. Note that for $z_0=0$ the force component in the v direction is infinite, because this represents an infinitely wide finger.

Formally it is possible to express the force directly by the w space in a transcendental equation thus omitting z_0. Let F_v be the force component directed at $-\mathrm{i}$, then by substituting the value of $(1-z_0)^{1/2}$ from Eq. (15) in Eq. (2) one obtains:

$$
\tanh\left(\pi\frac{F_v h}{\varepsilon V^2}\right)-\pi\frac{F_v h}{\varepsilon V^2}+\frac{\pi}{2}\frac{a}{h}=0. \tag{16}
$$

However, one may find the use of the two Eqs. (2) and (15) more practical than Eq. (16).

2.2.2. Case 2

Let the geometry of a long moving finger within the stator be simplified to half a rectangular finger adjacent to a rectangular chassis charged by electric potential. Assuming as previously a width of $2a$, a distance of $b\sim h$ to the wall and a distance h between the rod and the base illustrated in Fig. 2b, w maps to the upper half of a plane z via the Schwartz–Christoffel derivative $\mathrm{d}w/\mathrm{d}z$, such that

$$
\frac{\mathrm{d}w}{\mathrm{d}z}=B\frac{\sqrt{z+1}}{z\sqrt{z-1}}, \tag{17}
$$

where B is a constant. Assuming values of $w=0$ at $z=-1$, i.e. the origin of w lies at the tip of the moving finger, and $w=h(1+\mathrm{i})$ at $z=1$ the integral results in

$$w(u,v) = h\left\{ \frac{1+\mathrm{i}}{2} - \frac{\mathrm{i}}{\pi}\left[-\sin^{-1}\left(\frac{1}{z}\right) + \mathrm{i}\sin^{-1}(z)\right]\right\}, \tag{18}$$

where $z = x + \mathrm{i}y$, and $w = u + \mathrm{i}v$.

Determined by the geometry B becomes $\mathrm{i}h/\pi$. The boundary values apply such that $\phi = 0$ at $z < 0$, and $\phi = V$ at $0 < z$. Next the z plane, shown in Fig. 3b, is mapped to a plane η via $\eta = \ln(z)$ thus forming an infinite strip as shown in Fig. 3c. The boundary values apply such that $\phi = 0$ at $\mathrm{Im}(\eta) = -\pi$ and $\phi = V$ at $\mathrm{Im}(\eta) = 0$.

Following the procedure in case 1 one arrives at the following expression for the force per depth unit:

$$F = -\frac{\varepsilon}{2}\left(\frac{V}{\pi}\right)^2\left(\int_{\mathrm{i}0}^{\mathrm{i}H}\frac{z-1}{z+1}\,\mathrm{d}w - \mathrm{i}\int_a^0 \frac{z-1}{z+1}\,\mathrm{d}w\right), \tag{19}$$

whereby the normalized force after carrying out the integral becomes

$$2\frac{Fh}{\varepsilon V^2} = \frac{1}{2} + \frac{1}{\pi}\left(\cosh^{-1} z_1 - \sin^{-1}\frac{1}{z_1}\right) - \mathrm{i}\left[\frac{1}{2} + \frac{1}{\pi}\left(\cosh^{-1}\frac{1}{z_0} - \sin^{-1} z_0\right)\right], \tag{20}$$

where z_0 and z_1 of the z plane correspond to a and $\mathrm{i}H$ in the w plane, and are found from Eq. (18). The resulting force shows a component dependent on z_0 in the negative direction of $v(-\mathrm{i})$, and a component dependent on z_1 in the positive direction of u. Implied in Eq. (18) is that the integral is over the conformally transformed domain z rather than over w, omitting the problem of singularity at $w = 0$. Note the full symmetry of the solution allowing a system rotation by 90°.

Again, it is possible to express the force by the w space directly in a transcendental equation thus omitting z_0 and z_1. Let F_v be the force component directed at $-\mathrm{i}$, then by substituting the value of z_0 and z_1 from Eq. (18) in Eq. (19) one arrives at

$$2\frac{F_v h}{\varepsilon V^2} - \frac{2}{\pi}\cosh^{-1}\left\{\sec\left[\frac{2}{\pi}\left(2\frac{F_v h}{\varepsilon V^2} + \frac{a}{h}\right)\right]\right\} - \frac{a}{h} + 1 = 0. \tag{21}$$

2.2.3. Case 3

This case, illustrated by Fig. 2c, is treated in the section for case 1 concentrating on the force in the positive direction of u. As derived in Eq. (15), the normalized force is a unity, identical to a direct solution of the finger capacitor.

3. Results and discussion

The normalized force, for $b : a = 3.5 : 1.5$, acting on the moving finger $2Fb/\varepsilon V^2$ in the three solved cases is plotted against the normalized engagement distance $\delta/b = (\delta_0 - h)/b$ in Fig. 4, where δ_0 is the full motion stroke. Case 1 is the monotonously growing curve, case 2 is the point at $h = b$ or $\delta_0/b - 1$, and case 3 is the horizontal curve. Because each case represents only a limited range within the path of the moving finger, it is necessary to combine them in order to produce an expression compatible with the entire motion stroke. One considers the following phenomena: (1) on increasing h and approaching the point $h = b$ case 1 begins to underestimate the actual force, and (2) on increasing δ and approaching $h = b$ case 3 begins to underestimate the actual force.

Essentially, the force of case 1 becomes gradually less dominant as the finger moves away from the immediate proximity to the stator base where the effect of the force of case 3 is small. Then, the latter force begins to dominate when the finger moves to the far zone from the stator base. At the point $h = b$ case 2 is the true solution. Therefore, the force throughout the moving region can be expressed as

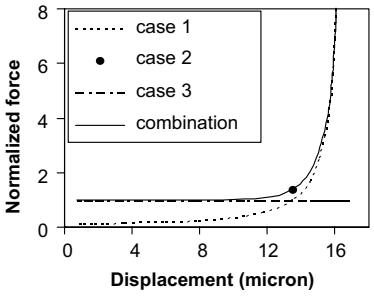

Fig. 4. The normalized force acting on the moving finger for $h = b$: (a) cases 1 and 3 are represented by the broken line and case 2 is the single circle, and (b) the combined force due to Eq. (22) is represented by the solid line.

$$\frac{2Fb}{\varepsilon V^2} = \alpha(\delta) + \beta(\delta) \ln \frac{1 - \sqrt{1 - z_0}}{1 + \sqrt{1 - z_0}}, \tag{22}$$

where α and β are weight functions. What one must reckon with is that the forces for cases 1 and 3 dominate specific respective regions, while outside of those regions their effect is negligible. Considering the decaying contributions of these forces on departing from their domination zones, these functions may be assumed to follow an *arctan* pattern, such that

$$\alpha(\delta) = \frac{1}{2} + \frac{1}{\pi} \tan^{-1} \frac{\delta_1 - \delta}{\Delta_1} \tag{23}$$

and

$$\beta(\delta) = \frac{1}{2} + \frac{1}{\pi} \tan^{-1} \frac{\delta - \delta_2}{\Delta_2}, \tag{24}$$

where the constants δ_1, δ_2, Δ_1, Δ_2 are obtained from the force values at $h = b$, in the case 1 zone $h < b$, and in the case 3 zone $h > b$. Further assumed is that case 1 ends at $h = b/3$ and case 3 begins at $h = 3b$ where the combined expression is evaluated at 99% of the case 3 magnitude. The combined calculation for the three cases due to Eq. (22) is also shown in Fig. 4. Observe that the curves up to $h = 3b$ and from $h = b/3$ overlap closely cases 3 and 1, respectively, while case 2 is always fully maintained.

The calculation is plotted in Fig. 5 in comparison with a finite-elements calculation. An excellent agreement is found between the theory and the numerical calculations. Then the analytical solution is plotted in Fig. 6 with b to a ratio as a parameter. The corresponding values of the constants δ_1, δ_2, Δ_1, Δ_2 are given in Table 1.

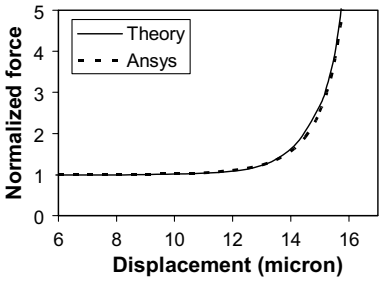

Fig. 5. Analytical result compared with a finite-elements calculation. The parameters are: $a = 1.5$ μm, $b = 3.5$ μm.

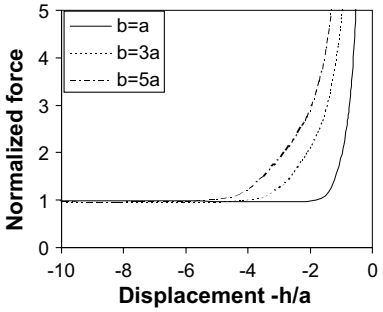

Fig. 6. Force predictions versus a moving finger displacement for $b = a$, $3a$ and $5a$.

Table 1
Values of parameters δ_1, δ_2, Δ_1, Δ_2, given in μm, for a number of gap-to-half finger-width $b : a$ ratios

$b : a$	δ_1	δ_2	Δ_1	Δ_2
1:1	16.84	15.83	0.45	0.29
2:1	16.52	15.96	0.32	0.25
3:1	15.99	14.19	0.76	0.59
5:1	15.16	13.40	0.83	0.72
3.5:1.5	15.40	13.49	1.13	0.88

4. Conclusions

A simple expression for the electrostatic force of a comb-drive moving-finger for the full stroke has been derived analytically. It covers the displacement path up to a nearly complete attachment to the stator basis. The normalized force equals unity up to the point $\delta/b = \delta_0/b - 3$, then it grows up to the point $\delta/b = \delta_0/b - 1/3$, then it escalates rapidly. Traditionally only the first of these zones, of the constant normalized force, has been controllably used in MEMS devices. Once an algebraic formula for the force is at hand, it can be used in the equation of motion to generate a transfer function valid throughout the entire engagement path. Hence the controllable motion stroke can be extended to include also the range where the force escalates approaching the "pull-in" region. Alternately, the nonlinear condition predicted by the model identifies the instability region of comb-drive actuators.

References

Brown, J.W., Churchill, R.V., 1995. Solution of electrostatic field potential for comb-drive actuators—analysis. In: Complex Variables and Applications, sixth ed. McGraw-Hill, NY.

Driscoll, T.A., 1996. Algorithm 756: A MATLAB toolbox for Schwartz–Christoffel mapping. ACM Trans. Math. Softw. 22 (June), 168–186.

Driscoll, T.A., 1999. Schwartz–Christoffel toolbox user's guide: version 2.1. Dept. Appl. Math., Univ. Colorado, Bolder, CO.

Goano, M., Bertazzi, F., Caravelli, P., Ghione, G., Driscoll, T., 2001. A general conformal-mapping approach to the optimum electrode design of coplanar waveguides with arbitrary cross section. IEEE Trans. Microwave Tech. 49, 1573–1580.

Jensen, B.D., Multu, S., Miller, S., Kurabayashi, K., Allen, J.J., 2001. Design and simulation of shaped comb fingers for compensation of mechanical restoring force in tunable resonators. In: Proc. 2001 ASME Int. Mechanical Engineering Congress and Exposition, New York, pp. 1–23.

Kim, C.J., Pisano, A.P., Muller, R.S., Lim, M.G., 1990. Polysilicon microgrippers. In: Tech. Dig. IEEE Solid-State Sensor and Actuator Workshop, Hilton Head, SC, pp. 48–51.

Pisano, A.P., 1989. Resonant—structure micromotors. In: Proc. IEEE Electro-Mechanical Syst. Workshop, Napa Valley, CA.

Sniegowski, J.J., Garcia, E.J., 1996. Surface-micromachined gear trains driven by an on-chip electrostatic micro-engine. IEEE Electron. Dev. Lett., 366–368.

Tang, W.C., Nguyen, T.H., Judy, M.W., Howe, R.T., 1990. Electrostatic comb drive of lateral polysilicon resonators. Sens. Actuators A 21–23, 328–331.

Wang, K., Nguyen, C.T.-C., 1999. High-order medium frequency micromechanical electronic filters. J. MEMS 8, 534–557.

Yao, J.J., Arney, S.C., MacDonald, N.C., 1992. Fabrication of high frequency two-dimensional nanoactuators for scanned probe devices. In: Proc. IEEE MEMS, pp. 14–22.

Ye, W., Mukherjee, S., MacDonald, N.C., 1998. Optimal shape design of an electrostatic comb drive in micromechanical systems. IEEE J. Michromech. Syst. 7, 16–25.

Yun, W., Howe, R.T., Gray, P.R., 1992. Surface micromachined, digitally force-balanced accelerometer with integrated CMOS detection circuitry. In: Tech. Dif. IEEE Solid-State and Actuator Workshop, Hilton Head, SC, pp. 126–131.